
A Search for Faint Planetary Nebulae Using the DSS

G.H. Jacoby¹, M. Kronberger², D. Patchick², P. Teutsch², J. Saloranta², A. Acker³, and D. Frew⁴

¹ WIYN Observatory jacoby@wiyn.org,

² Deep Sky Hunters <http://groups.yahoo.com/group/deepskyhunters>,

³ Strasbourg Observatory acker@newb6.u-strasbg.fr,

⁴ Macquarie/Perth David.Frew@dec.wa.gov.au

Summary. A group of amateur astronomers (Deep Sky Hunters) has identified ~ 50 candidate PNe by visually searching the 1st and 2nd generation red Digital Sky Survey images. Candidate PNe are then observed in H α with larger telescopes, primarily the WIYN 3.5-m on Kitt Peak, and the 1.2-m and 1.5-m at Haute-Provence Observatory (OHP). Thus far, ~ 20 new PNe have been found. These objects have a strong tendency to have low surface brightness and to be relatively round.

Key words: Planetary nebulae, Digital sky survey

1 Introduction and Methodology

Predictions for the number of PNe in the Galaxy (8,000 to 140,000 [2, 3, 9, 10, 11]), greatly exceed the number known ($\sim 2,500$ [8]), even for optimistic estimates of both numbers. The factor of 3 to 55 discrepancy can be explained in several ways:

1. Extinction in the Galactic plane obscures a great majority of PNe.
2. Survey techniques are biased against finding most PNe (e.g., DSS searches do not identify stellar PNe).
3. Rapid evolution makes most of the PNe fainter than we think.
4. There are far fewer PNe in the Galaxy than implied by the estimates, perhaps due to errors in distances or stellar evolution scenarios.

Each of these explanations carries a significant and problematic set of implications. For example, the latter two ideas demand a change in our understanding of stellar evolution; the last item, in particular, can be understood if PNe can only form from an interacting binary star scenario [7]. Thus, a count of the true number of PNe in the Galaxy may provide a direct test of the predictions of the theories of stellar physics.

There are many ways to search for PNe in the Galaxy to improve the number count. We describe one method here, along with results from a preliminary survey. In this method, amateur astronomers ("The Deep Sky Hunters" or DSH) identify

PNe, primarily at Galactic latitudes between 5 and 10 degrees (north and south), by visually searching the 1st and 2nd generation red Digital Sky Survey images, sometimes along with 2MASS [6]. Candidates are checked for reality in other DSS colors and compared with SIMBAD, NED and VIZIER to ensure that they are new.

Objects are selected by their morphology and compared to near-IR DSS images that are primarily continuum, to improve the sensitivity to H α + [NII] emission. The best candidates are then imaged in H α with other telescopes, primarily the WIYN 3.5-m on Kitt Peak and the 1.2-m and 1.5-m at OHP.

2 Observations and Results

About 50 candidate PNe were identified by the DSH group, and 25 candidates were observed with CCD imagers on the other telescopes. Observations consist of 300 sec snapshots at WIYN (200 sec at OHP) using a narrow-band filter to isolate H α + [N II]. The imager at WIYN is the 4K x 4K OPTIC CCD camera [1]. In some cases, an [O III] image or a spectrum (Pa 1, Te 8) were obtained, but those situations are rare.

Based on morphological and emission-line characteristics, 13 candidates are classified as new PNe. Eight additional candidates are probably PNe, while four are unlikely to be PNe. The "yield" rate of $\sim 70\%$ demonstrates that the method is effective and rewarding. Morphology alone is not always a reliable criterion to classify an emission-line object as a PN. Therefore, the color of the apparent central star is examined, and if found to be very blue (column 5 of Table 1.1), provides additional evidence for the PN classification. Ultimately, a spectrum of each object is needed. For this interim report, we base our classification mostly on morphology and central star color, dividing the candidates into 2 classes - probable (Figure 1.1), and possible (Figure 1.2). Some subjectivity is inevitable in this approach, and several "possible" candidates could have been assigned to the "probable" group. In fact, some members of our team preferred moving Kn 2, 39, and 40 into the "probable" group. Table 1.1 lists the candidates with their coordinates. Kn 21, Pa 1, Pa 2, Pa 5, Pa 6, and Te 8 had been suspected previously [6] as being PNe.

The two chief characteristics of the new PN candidates are that the objects have very low surface brightness, and that they tend to be more round than most PNe. In discussions at this meeting, there has been some suggestion that PNe become more round as they become older, based on a correlation between low surface brightness and roundedness (e.g., Abell 39 [4], PG 1520+525 [5]). If the correlation is a real physical phenomenon, the physics is yet to be understood. Alternatively, there may be a selection effect with this visual search technique that biases for finding faint PNe that are round.

Acknowledgement. We wish to thank Robin Ciardullo, Steve Howell, and Kim Herrmann for their assistance at WIYN in acquiring the H α + [N II] images of the PN candidates, and Jean-Francois Soulier and the BEATEP students for acquiring images and spectra at OHP.

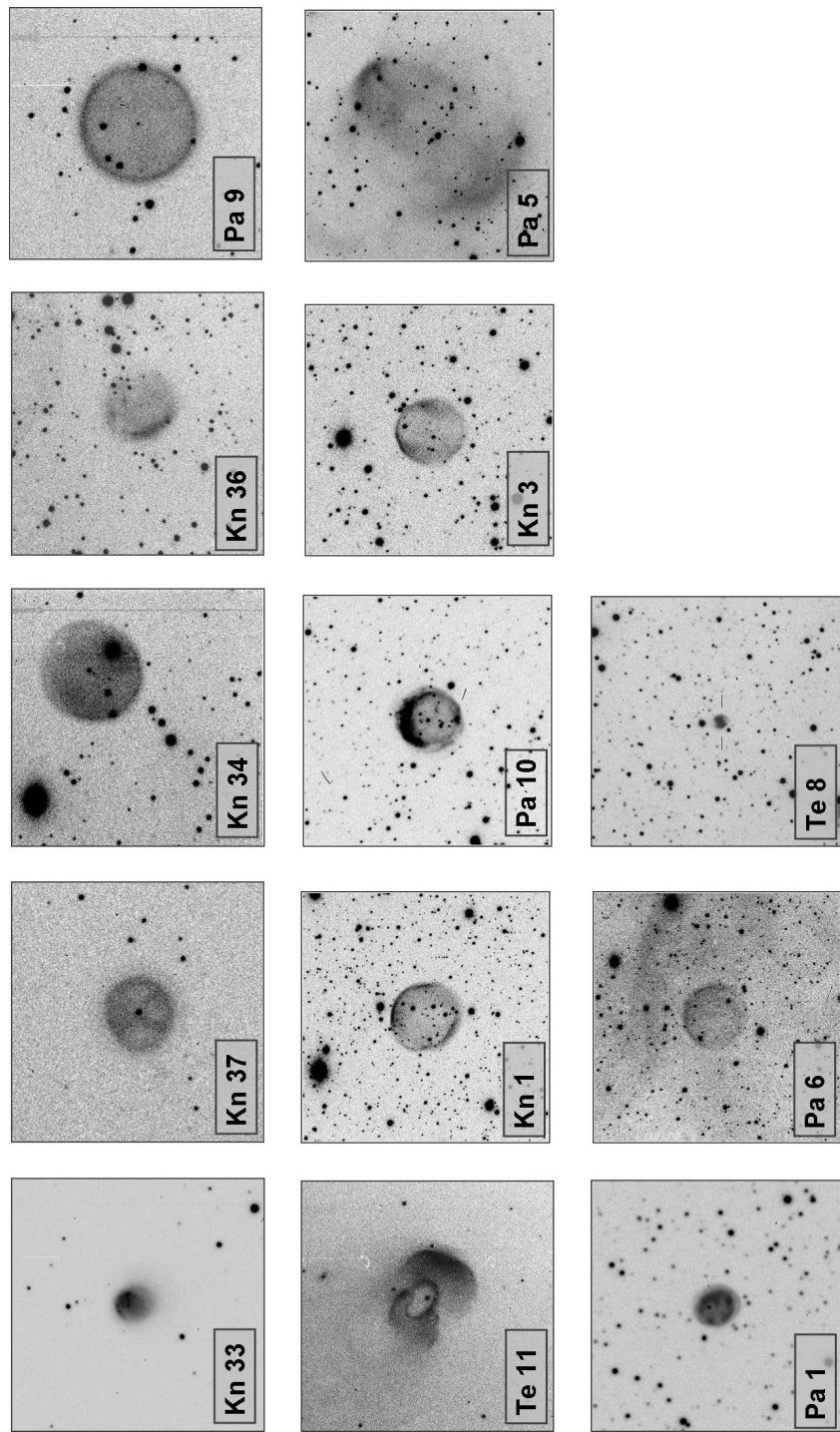


Fig. 1. The 13 “probable” PN candidates. North is left, east is down on the page. Each box is a different size - see Table 1.1 for the scale size of each box.

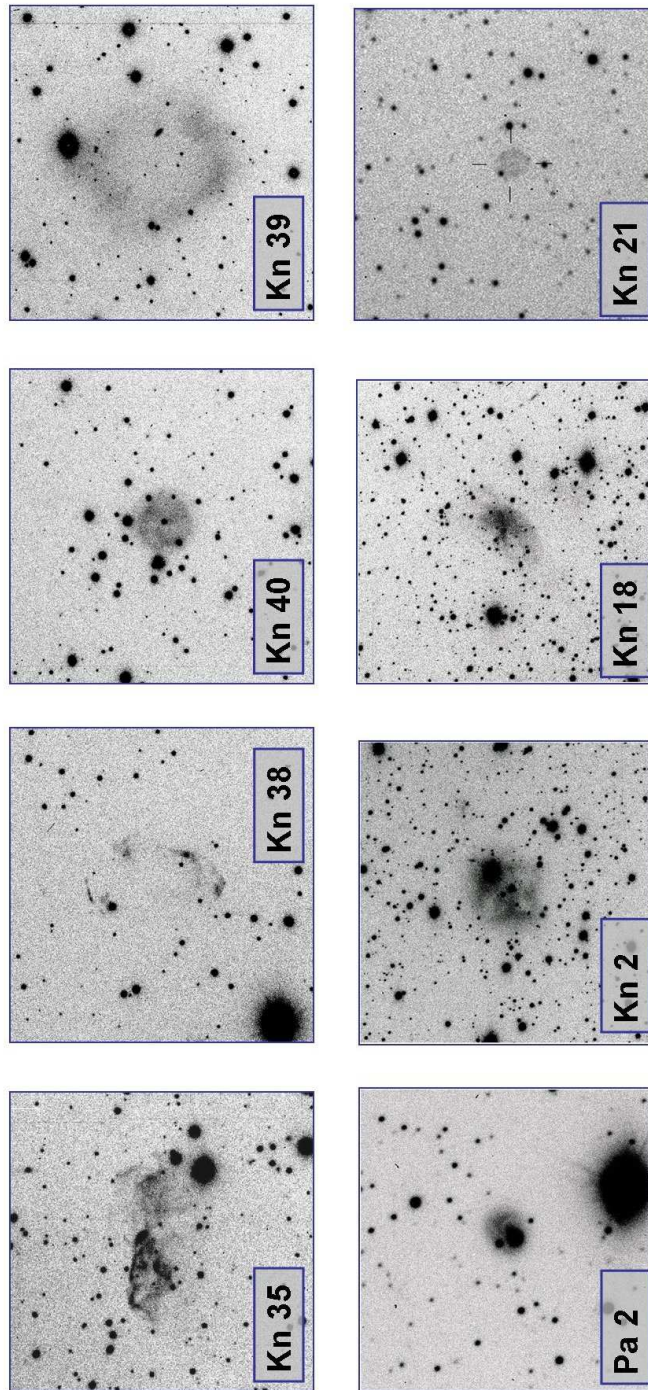


Fig. 2. The 8 “possible” PN candidates. North is left, east is down on the page. Each box is a different size - see Table 1.1 for the scale size of each box.

Table 1. Properties of the New PN Candidates

Object	RA (2000)	Dec (2000)	Box Size (arcmin)	Blue CS (on DSS)	Size (AxB) (arcsec)
Kn 33	04:32:38.1	+60:20:12	1.6	Y	17x16
Kn 37	04:44:37.8	+37:39:15	1.3	Y	31x28
Kn 34	04:45:18.7	+59:09:24	2.5	Y	60x57
Kn 36	04:55:24.5	+52:59:15	3.3		59x50
Kn 35	04:55:25.0	+53:14:05	3.3		106x66
Kn 38	05:16:16.5	+27:27:19	2.6		70x46
Pa 9	05:37:58.0	+17:06:18	1.7	Y	53x53
Te 11	05:45:58.3	+02:21:06	1.6		43x34
Kn 40	06:00:47.2	+09:28:40	2.7	Y	37x37
Kn 39	06:59:23.8	+18:26:49	3.3	Y	111x102
Pa 2	17:14:48.9	-14:15:54	1.4		16x13
Kn 2	18:32:40.0	+13:58:02	3.0	Y	56x52
Kn 1	18:35:51.5	+10:57:19	2.9	Y	57x53
Pa 10	18:37:10.7	+04:28:17	1.5		27x26
Kn 3	18:55:21.8	+15:11:44	1.5		29x28
Pa 5	19:19:30.6	+44:45:44	3.0	Y	157x154
Kn 18	19:24:06.9	+33:52:10	2.9		64x27
Pa 1	19:47:02.7	+29:30:26	1.2		14x12
Pa 6	20:09:40.9	+41:14:43	2.9	Y	48x48
Kn 21	20:41:18.0	+27:35:06	3.8	Y	29x25
Te 8	20:55:27.3	+39:03:57	5.2		23x18

References

1. S.B. Howell et al: *PASP*, **115**, 1340 (2003)
2. K. Ishida and R. Weinberger: *A&A*, **178**, 227 (1987)
3. G.H. Jacoby: *ApJS*, **42**, 1 (1980)
4. G.H. Jacoby, G.J. Ferland, and K.T. Korista: *ApJ*, **560**, 272 (2001)
5. G.H. Jacoby, and G. van de Steene: *AJ*, **110**, 1285 (1995)
6. M. Kronberger et al: *A&A*, **447**, 921 (2006)
7. M. Moe and O. De Marco: *ApJ*, **650**, 916 (2006)
8. Q.A. Parker et al: in *IAU Symp* **209**, 25 (2003)
9. M. Peimbert: *Rev. Mex. AA*, **20**, 119 (1990)
10. J.P. Phillips: *ApJS*, **139**, 199 (2002)
11. S.R. Pottasch: *A&A*, **307**, 561 (1996)